Table I. Substituent Effect on First-Order Rate Constants for the Heterolytic O–O Bond Cleavage of **4** in CH_2Cl_2 at −80 °C

compds[b]	10^3k_{dec}, s^{-1} (log k_{rel}[c])	
	m-CPBA[d]	*p*-NO_2PBA[e]
4a	3.2 (0.00)	11.2 (0.00)
4b	0.7 (−0.64)	2.5 (−0.65)
4c	16.6 (0.72)	50.8 (0.66)
4d	4.0 (0.10)	14.5 (0.11)
4e	*a*	0.6 (−1.28)
4f	0.5 (−0.77)	2.2 (−0.71)

[a] Not available. [b] See Figure 1. [c] k_{rel} is the relative rate constant based on that of **4a**. [d] 3 equiv of *m*-chloroperoxybenzoic acid were used. [e] 3 equiv of *p*-nitroperoxybenzoic acid were used.

2. Furthermore, a possible intermediate, **2** or **2'**, has never been observed in these catalytic systems.

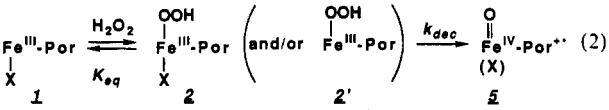

$$k_{obs} = k_{dec}[\mathbf{2}\ (\text{or}\ \mathbf{2'})] = k_{dec}{\cdot}K_{eq}[\mathbf{1}][H_2O_2]$$

In order to understand the push effect on the O–O bond cleavage reaction of the (hydroperoxo)iron(III) porphyrin complex, we have examined the reactivity of a series of (acylperoxo)iron(III) porphyrins (**4**) by changing substituents at the *meso* positions of the porphyrin ring. The substituted porphyrins listed in Figure 1 were prepared according to the methods reported.[10]

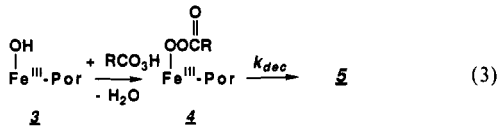

In a typical reaction, a methylene chloride solution of hydroxoiron porphyrin (**3b**, 2.0×10^{-5} M) was cooled to −80 °C in a UV–vis cuvette. Introduction of 3 equiv of *p*-nitroperbenzoic acid to the solution immediately afforded (acylperoxo)iron(III) porphyrin (**4b**), which exhibits a typical visible spectrum for five-coordinated high-spin iron(III) porphyrins but different from that for the hydroxide complex (Figure 2).[11] The following transformation of **4b** to an oxoferryl porphyrin cation radical[12] (**5b**) was also directly observed as shown in Figure 2. Trace A in Figure 2 shows the time course of absorbance change of **3b** at 415 nm upon the addition of 3 equiv of *p*-nitroperoxybenzoic acid. Similar spectral changes were also observed in the reaction of **3a,c–f** with peracids under the conditions described above. From an analysis of the spectral changes, the O–O bond cleavage of **4** was found to be first-order in [**4**] ($d[\mathbf{5}]/dt = k_{dec}[\mathbf{4}]$) as shown in Figure 2 (inset), consistent with recent observation by Groves and Watanabe.[13] Values of the rate constants (k_{dec}) for several substituted porphyrins are summarized in Table I. As expected for the heterolytic O–O cleavage in **4**, *p*-nitroperbenzoato)iron(III) porphyrin complexes decompose faster than the *m*-chloroperbenzoate derivatives (pull effect).[13,14] At the same time, electron-donating groups at the *meso* positions of a porphyrin ring were found to accelerate the O–O bond cleavage step, whereas

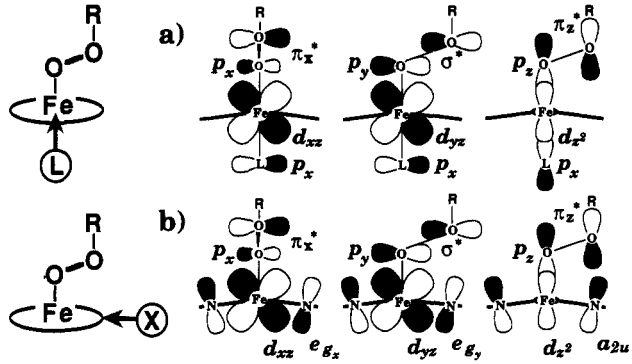

Figure 3. Idealized orbital interaction diagrams for peroxoiron(III) porphyrin complexes: (a) interaction among the sixth ligand's p orbitals, iron d orbitals, and peroxo p orbitals; (b) interaction among the porphyrin ligand's orbitals, iron d orbitals, and peroxo p orbitals.

electron-withdrawing substituents retarded the formation of **5**. A Hammett plot of log k_{rel} vs the summation of Hammett σ's of the substituents gives a slope ρ of −0.53 (correlation coefficient: 0.92). These observations demonstrate that the electron donor at the *meso* positions of a porphyrin ring accelerates the heterolytic O–O bond cleavage reaction effectively.

Implication of the Push Effect of Substituents on a Porphyrin Ring. Figure 3 shows the orbital interaction diagrams among iron, porphyrin, axial ligand, and peroxide. The oxygen p orbitals (σ^* and π^*) of the iron-bound peroxide are overlapped with iron d_{xz}, d_{yz}, and d_{z^2} orbitals, which also interact with the p orbitals of an axial ligand (Figure 3a). Thus, the push effect by the axial ligand on the heterolytic O–O bond cleavage depicted in eq 1 can be explained by the orbital interaction between the ligand and peroxide through iron. Since the porphyrin e_g and a_{2u} orbitals on the pentacoordinated domed porphyrin ring, in which large electron densities are localized at the pyrrole nitrogens and the *meso* carbons, interact with iron d_{xz}, d_{yz}, and d_{z^2} orbitals, *meso* substituents on a porphyrin ring as well as the axial ligand are also expected to affect the rate of the heterolytic O–O bond cleavage. These considerations are consistent with the experimental results shown in Table I.

In conclusion, it has been shown that the internal electron donor to destabilize the O–O bond (push effect) is important in the heterolytic O–O bond cleavage process of *meso*-substituted (acylperoxo)iron(III) porphyrin complexes to form the corresponding oxoiron(IV) porphyrin cation radicals.

Division of Molecular Engineering
Graduate School of Engineering
Kyoto University
Kyoto 606, Japan

Kazuya Yamaguchi
Yoshihito Watanabe
Isao Morishima*

Received October 30, 1991

(10) (a) Lindsey, L. S.; Wagner, R. W. *J. Org. Chem.* **1989**, *54*, 828–836. (b) Kobayashi, H.; Higuchi, T.; Kaizu, Y.; Osada, H.; Aoki, M. *Bull. Chem. Soc. Jpn.* **1975**, *48*, 3137.
(11) (a) Woon, T. C.; Shirazi, A.; Bruice, T. C. *Inorg. Chem.* **1986**, *25*, 3845–3846. (b) Groves, J. T.; Watanabe, Y. *Inorg. Chem.* **1987**, *26*, 785–786.
(12) Formation of oxoferryl porphyrin cation radicals was also confirmed by NMR spectroscopy in comparison with the result of Groves et al.; see ref 15.
(13) Groves, J. T.; Watanabe, Y. *J. Am. Chem. Soc.* **1988**, *110*, 8443–8452.
(14) Lee, W. A.; Bruice, T. C. *J. Am. Chem. Soc.* **1985**, *107*, 513–514.
(15) (a) Groves, J. T.; Haushalter, R. C.; Nakamura, M.; Nemo, T. E.; Evans, B. J. *J. Am. Chem. Soc.* **1981**, *103*, 2884–2886. (b) Gold, A.; Jayaraj, K.; Doppelt, P.; Weiss, R.; Bill, E.; Ding, X.-Q.; Bominaar, E. L.; Trautwein, A. X.; Winkler, H. *New J. Chem.* **1989**, *13*, 169–172.

Environmentally Induced Multiple Intervalence Transitions in a Symmetrically Substituted Analogue of the Creutz–Taube Ion

Intervalence transition energies for class II (valence localized) mixed-valence systems are known to be a sensitive function of molecular environment[1] (i.e. solvent,[2] ionic strength,[3-5] etc.). Class

(1) For a general review, see: Creutz, C. *Prog. Inorg. Chem.* **1983**, *30*, 1.
(2) See, for example: Brunschwig, B. S.; Ehrenson, S.; Sutin, N. *J. Phys. Chem.* **1986**, *90*, 3657 and references therein.
(3) (a) Hammack, W. S.; Drickamer, H. G.; Lowery, M. D.; Hendrickson, D. N. *Chem. Phys. Lett.* **1986**, *132*, 231. (b) Lowery, M. D.; Hammack, W. S.; Drickamer, H. G.; Hendrickson, D. N. *J. Am. Chem. Soc.* **1987**, *109*, 8019.

0020-1669/92/1331-0157$03.00/0

III (valence delocalized) transitions, on the other hand, are largely insensitive to the detailed nature of the surroundings.[1,6] We wish to report here a very unusual environmental effect: the appearance of multiple intervalence bands in response to both solvent and added electrolyte. The molecular system exhibiting the effect is *trans*-(py)$(NH_3)_4$Ru–pz–Ru$(NH_3)_4$(py)$^{5+}$ (**1**)—a borderline class II/class III system[7,8] and a close structural analogue of the well-known Creutz–Taube ion, $(NH_3)_5$Ru–pz–Ru$(NH_3)_5^{5+}$ (py is pyridine; pz is pyrazine).[9] Interestingly, the C-T ion itself (a class III system) does not display the effect, nor does a fully class II analogue, $(NH_3)_5$Ru–4,4′bpy–Ru$(NH_3)_5^{5+}$ (although other environmental effects are known for the bpy-bridged ion[5c,10]).

As shown by Figure 1, a single intervalence transition exists for **1** in pure acetonitrile as solvent.[11] (The same behavior is seen in other single-component solvents.[12]) Addition of small amounts of dimethyl sulfoxide (DMSO), however, leads initially to a shoulder on the higher energy side and eventually to a second full intervalence band, some 1300 cm^{-1} to the blue of the original. Further additions of DMSO (Figure 1) ultimately lead to recovery of a single transition, with an energy and shape almost indistinguishable from the original.

In our earliest experiments we found the band multiplicity effects in Figure 1 difficult to reproduce, at least in a quantitative sense. Eventually we discovered that the concentration of counterion (either from the chromophore and any needed oxidant or simply from added "inert" electrolyte) played a highly significant role in modulating the intervalence effect. Figure 2 summarizes a large number of experiments in which both the solvent composition and the counterion concentration (PF_6^-) have been varied. In the figure, the overall width at half-height ($\Delta\bar{\nu}_{1/2}$) for the intervalence absorption envelope (one or two transitions) is presented as a function of mixed-solvent composition for a range of initial hexafluorophosphate counterion concentrations. The most notable features of the plot are that the band broadening (or multiplicity) effect is most significant at the highest PF_6^- concentrations and that the effect maximizes (for most PF_6^- concentrations) after addition of just 0.8 mol % of DMSO.

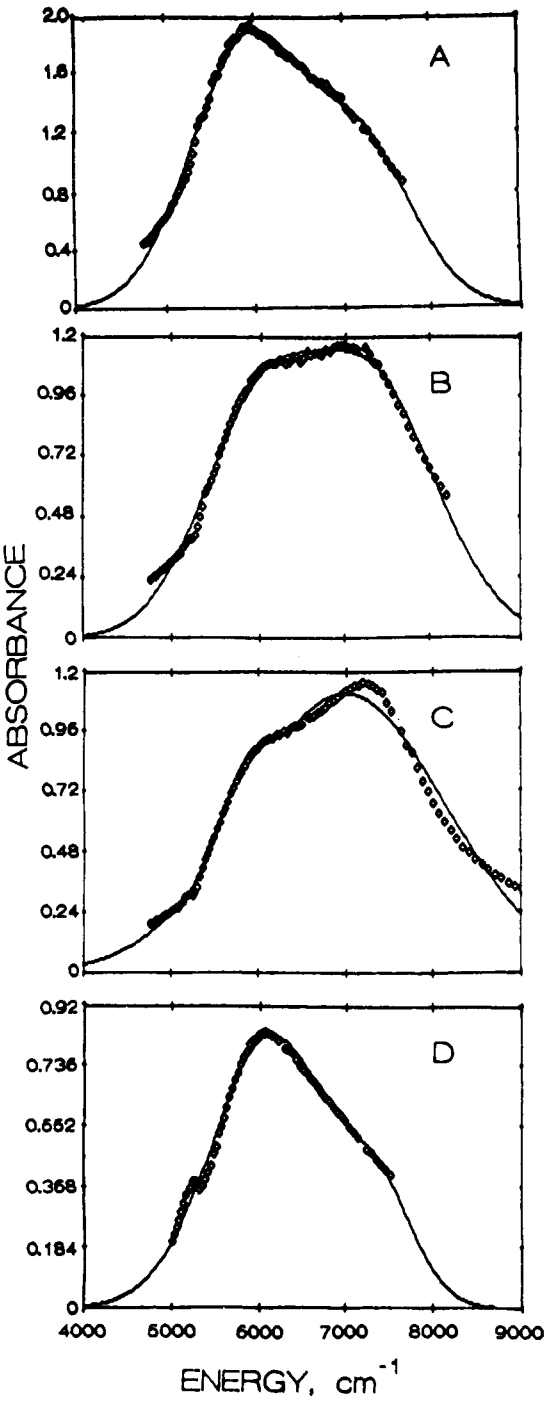

Figure 1. Intervalence absorption spectra for *trans*-(py)$(NH_3)_4$Ru(pz)-Ru$(NH_3)_4$(py)$^{5+}$ (oxidized with $[Fe(bpy)_3](PF_6)_3$) in acetonitrile/DMSO mixtures: (A) 0 mol % DMSO; (B) 0.8 mol % DMSO; (C) 2.0 mol % DMSO; (D) 50 mol % DMSO. The chromophore concentration is 0.63 mM. The absorbance is corrected for dilution. Solid lines represent arbitrary fitting of data to two Gaussians. (The difference in absorbance between panels A and D appears to reflect, in part, unintended reduction of the mixed-valence ion (presumably by trace impurities); the absorbance in (D) is increased upon further addition of oxidant.)

To the best of our knowledge, only three other reports of intervalence multiplicity exist.[13-15] Two of these concern ligand-bridged osmium dimers (class II as well as class III) for which large spin–orbit coupling effects exist.[13,14] The coupling gives rise

(4) (a) Lewis, N. A.; Obeng, Y. S. *J. Am. Chem. Soc.* **1988**, *110*, 2307. (b) Lewis, N. A.; Obeng, Y. S.; Purcell, W. L. *Inorg. Chem.* **1989**, *28*, 3796.

(5) (a) Blackbourn, R. L.; Hupp, J. T. *Chem. Phys. Lett.* **1988**, *150*, 399. (b) Blackbourn, R. L.; Hupp, J. T. *J. Phys. Chem.* **1990**, *94*, 1788. (c) Blackbourn, R. L. Ph.D. Dissertation, Northwestern University, 1991.

(6) See, for example: (a) Hammack, W. S.; Lowery, M. D.; Hendrickson, D. N.; Drickamer, H. G. *J. Phys. Chem.* **1988**, *92*, 1771. (b) Creutz, C.; Chou, M. H. *Inorg. Chem.* **1987**, *26*, 2995.

(7) [*trans*-(py)$(NH_3)_4$Ru–pz–Ru$(NH_3)_4$(py)]$(PF_6)_4$ was prepared as follows: Typically, a 3–4-fold molar excess of [*trans*-(py)$(NH_3)_4$Ru-$(H_2O)](PF_6)_2$ (200–300 mg) (Chang, J. P.; Fung, E. Y.; Curtis, J. C. *Inorg. Chem.* **1986**, *25*, 4233) was stirred with an appropriate quantity of pyrazine in deoxygenated (argon saturated) acetone for 4–5 h at room temperature. The purple product was precipitated by adding the reaction solution to 20 volumes of cold, stirring diethyl ether. The ether was removed by filtration and the solid product dried. The product was purified by metathesis (PF_6^- to Cl^- to PF_6^-) and by recrystallization at 0 °C from toluene/acetone mixtures (see: Chang et al). Product purity was judged chiefly by electrochemical measurements (which are exceptionally sensitive to both monomeric and oxo-bridged oligomeric ruthenium ammine species). Satisfactory elemental analyses (C, H, N) were obtained. The mixed-valence (5+) form of the dimer was generated in situ by using $[Fe(bpy)_3](PF_6)_3$ (bpy is 2,2′-bipyridine) as a stoichiometric oxidant. Agreement with previously reported spectroscopic and redox properties was obtained (De la Rosa, R.; Chang, P. J.; Salaymeh, F.; Curtis, J. C. *Inorg. Chem.* **1985**, *24*, 4231).

(8) Evidence for class III behavior comes chiefly from the narrow line shape, the insensitivity of the transition energy to solvent dielectric properties (in single-component solvents), and the structural similarity to the Creutz–Taube ion.

(9) Creutz, C.; Taube, H. *J. Am. Chem. Soc.* **1969**, *91*, 3988; **1973**, *95*, 1086.

(10) (a) Hupp, J. T.; Weydert, J. *Inorg. Chem.* **1987**, *26*, 2657. (b) Todd, M. D.; Dong, Y.; Hupp, J. T. *Inorg. Chem.*, in press.

(11) Intervalence absorption spectra were obtained by using matched 1-cm cells in a Perkin-Elmer 330 spectrophotometer.

(12) Curtis, J. C. Private communication.

(13) Kober, E. M.; Goldsby, N. A.; Narayan, D. N. S.; Meyer, T. J. *J. Am. Chem. Soc.* **1983**, *105*, 4303.

(14) Magnuson, R. H.; Lay, P. A.; Taube, H. *J. Am. Chem. Soc.* **1983**, *105*, 2507.

(15) Sinha, U.; Lowery, M. D.; Hammack, W. S.; Hendrickson, D. N.; Drickamer, H. G. *J. Am. Chem. Soc.* **1987**, *109*, 7340.

to exceptionally large splittings in the excited-state $d\pi(Os)$ manifold, which in turn leads to multiple intervalence transitions from a single ground electronic configuration.

The third report[15,16] involves the bis(fulvalene)diiron monocation—a known class III system. Here Hendrickson, Drickamer, and co-workers have observed an external pressure effect (for pure crystalline samples[17]) which leads, at a phenomenological level, to results which are remarkably similar to those in Figure 1. The interpretation is that two excited states (and one ground state) exist. Because of a differential effect of pressure upon electronic mixing, the relative intensities (and energies) for the two transitions evidently vary, leading to appreciably greater resolution of overlapping bands at certain pressures than at others.

For **1**, it is difficult to envision how the single ground-state/multiple excited-state model might be applicable. Spin–orbit energy effects, for example, are of roughly the right magnitude[18] but seem unlikely to respond in a dramatic way to external (environmental) perturbations.

An alternative hypothesis is that multiple *ground*-state forms of **1** exist, each featuring only one intervalence absorption. If correct, then the present results would be highly reminiscent of earlier findings for $(NH_3)_5Ru^{II}$–4,4′bpy–$Ru^{III}(NH_3)_5^{5+}$ (**2**).[5c,10] For **2**, intervalence blue shifts appear in mixed solvents[10a] or in the presence of added electrolyte.[5c] The shifts have been successfully interpreted in terms of a symmetry reduction effect[19] arising from selective solvation,[10a] or ion pairing,[5,6a] preferentially at the more highly oxidized metal center, leading to additional, energetically distinct ground-state forms of the mixed-valence ion. However, because the intervalence bands for **2** are broad ($\Delta\bar{\nu}_{1/2} \approx 5000\ cm^{-1}$), the presence of multiple chromophoric forms leads only to a widening and shift of the overall (structureless) absorption envelope. If a similar effect existed for **1**, then the much narrower line shape (see Figure 2) might well lead to spectral resolution of individual component chromophoric forms (Figure 1).

Given this hypothesis, one point is still potentially troubling:[20] there is an implicit assumption that, for a specific dimer, DMSO molecules and counteranions are somehow able to distinguish one redox trapping site from another. This in turn implies that some degree of charge differentiation or valence localization exists for the two nominally identical (i.e. class III) sites[8] within **1**. One possibility is that even within a predominantly class III system, enough residual polarization may exist to permit preferential solvation or ionic interactions at one or the other of the two available sites. Another is that the counterion or hydrogen-bond-accepting solvent molecule itself may provide the necessary electrostatic polarization to localize the valencies,[21] thereby permitting structural asymmetry within the second coordination sphere[19] (first solvation layer) and thus inducing a substantial blue shift in the intervalence absorption. While clearly speculative, the concept does have theoretical support.[22] Emerging experimental methodologies, such as extended near-infrared Raman scattering[23] and intervalence Stark spectroscopy,[24] should eventually permit us to test these or related hypotheses.

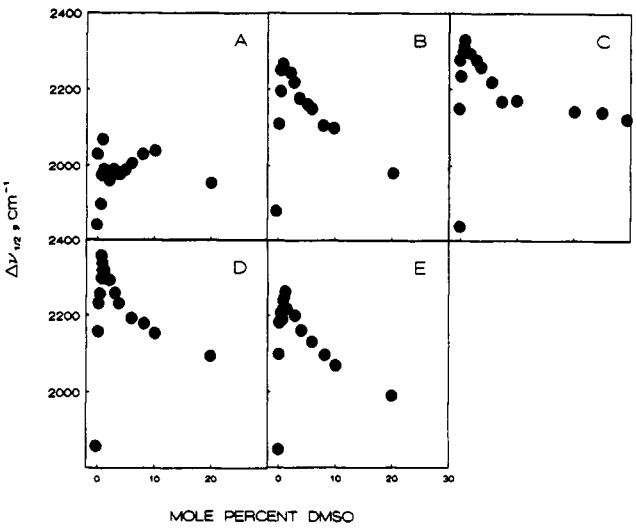

Figure 2. Change in full width at half-maximum of intervalence absorption band of **1** as a function of DMSO (solvent) and hexafluorophosphate (counterion) concentration: (A) $[PF_6^-] \approx 2.5$ mM, [dimer] = 0.40 mM; (B) $[PF_6^-] = 4.0$ mM, [dimer] = 0.17 mM; (C) $[PF_6^-] = 5.69$ mM, [dimer] = 0.16 mM; (D) $[PF_6^-] = 6.8$ mM, [dimer] = 0.16 mM; (E) $[PF_6^-] = 7.88$ mM, [dimer] = 0.16 mM. Sources of PF_6^-: (A) dimer and oxidant ($[Fe(bpy)_3](PF_6)_3$); (B–E) dimer, oxidant, and added tetrabutylammonium hexafluorophosphate.

(16) Mention should also be made of earlier work by Hendrickson and co-workers (*J. Chem. Phys.* **1973**, *59*, 380) and by Talham and Cowan (*Organometallics* **1984**, *3*, 1712), which was suggestive of multiple transitions for the bis(fulvalene)diiron cation (based on asymmetry in the intervalence line shape).

(17) Vestiges of the effect are observable in other media (see ref 15).

(18) Hupp, J. T.; Meyer, T. J. *Inorg. Chem.* **1987**, *26*, 2332.

(19) Specific examples of symmetry reduction based on second-sphere interactions would include $FcC{\equiv}CFc^+,PF_6^-$ (Fc is ferrocene; see ref 5) and $(1-x)CH_3CN,x$DMSO·$(NH_3)_5Ru^{II}$–4,4′bpy–$Ru^{III}(NH_3)_5$·yDMSO,$(1-y)CH_3CN$, where $x \neq y$ and where x, y, $(1-x)$, and $(1-y)$ signify fractional occupancies of the second sphere (see: ref 10a. Ennix, et al. *Inorg. Chem.* **1989**, *29*, 3791. Blackbourn, R. L.; Hupp, J. T. *Inorg. Chem.* **1989**, *29*, 3786). As suggested by eqs A and B, intervalence blue shifts can accompany symmetry reduction because of the finite optical energetic cost of incipient ion and/or solvent translation:

$$FcC{\equiv}CFc^+,PF_6^- \xrightarrow{h\nu} {}^+FcC{\equiv}CFc,PF_6^- \rightarrow PF_6^-,{}^+FcC{\equiv}CFc \quad (A)$$

$$(1-x)CH_3CN,x\text{DMSO}\cdot(NH_3)_5Ru^{II}\text{–}4,4'\text{bpy–}Ru^{III}NH_3)_5^{5+}\cdot y\text{DMSO},(1-y)CH_3CN \xrightarrow{h\nu} (1-x)CH_3CN,x\text{DMSO}\cdot(NH_3)_5Ru^{III}\text{–}4,4'\text{bpy–}Ru^{II}NH_3)_5^{5+}\cdot y\text{DMSO},(1-y)CH_3CN \rightarrow (1-y)CH_3CN,y\text{DMSO}\cdot(NH_3)_5Ru^{III}\text{–}4,4'\text{bpy–}Ru^{II}NH_3)_5^{5+}\cdot x\text{DMSO},(1-x)CH_3CN \quad (B)$$

For several examples involving solid-state mixed-valence chemistry, see: Hendrickson, D. *Comments Inorg. Chem.* **1985**, *4*, 329.

(20) One other potential point of concern is the apparent existence (very poorly resolved) of two intervalence components even in pure CH_3CN at low ionic strength (see panel A of Figure 1). One possible explanation for the two components would be vibronic structuring for a single electronic transition. Another might possibly be spin–orbit coupling, which could lead to modest splitting of the excited-state $d\pi(Ru)$ manifold and, therefore, multiple electronic transitions (see text). Regardless of which explanation is most appropriate, we tentatively interpret as coincidental the appearance of shoulders in panels A and D (Figure 1) at roughly the same energy as the peak in panel B. (Note, however, that we cannot completely rule out a common origin (such as a class II/class III equilibrium) for all of the various observed intervalence absorption structures (panels A–D).)

(21) A reviewer has asked us to comment on the possible relevance here of Kolling's work on nonideal static dielectric behavior for binary solvent mixtures (*Anal. Chem.* **1987**, *59*, 674; *J. Phys. Chem.* **1991**, *95*, 3950), a point Kolling has raised as well in a slightly different context (electrochemical experiments; see ref 19). Four observations argue against a significant role for dielectric nonideality in the present investigation: (1) The magnitude of Kolling's dielectric effect, while larger for DMSO/CH_3CN than for most other mixtures, is still fairly modest (maximum deviation of ca. 7% from ideal behavior). (2) The solvent composition dependence of the nonideal dielectric effect (i.e. broadly varying, with a maximum near 50 mol %) differs greatly from the narrow composition dependence found in Figure 2 and in related optical[5,10] and electrochemical[10,19] studies. (3) Selective solvation effects for a related cobalt ammine complex in several binary mixtures clearly correlate with differences in solvent Lewis base strength (Mayer; et al. *J. Electroanal. Chem. Interfacial Electrochem.* **1979**, *100*, 875), rather than with dielectric excess mixing parameters. (4) Non-ammine-bearing complexes fail to display selective solvation effects (optical[5b] or electrochemical[19]) in DMSO/CH_3CN mixtures. It seems clear that the unusual phenomena reported here, at least, derive from *specific* ligand/local-solvent interactions, rather than from bulk solvent nonidealities.

(22) Katriel, J.; Ratner, M. A. *J. Phys. Chem.* **1989**, *93*, 5065.

(23) For a preliminary report involving near-IR (rather then extended near-IR) resonance Raman, see: Doorn, S. K.; Hupp, J. T.; Porterfield, D. R.; Campion, A.; Chase, D. B. *J. Am. Chem. Soc.* **1990**, *112*, 4999.

(24) Oh, D. H.; Boxer, S. G. *J. Am. Chem. Soc.* **1989**, *111*, 1130.

Acknowledgment is made to the donors of the Petroleum Research Fund, administered by the American Chemical Society, for partial support of this research. Matching support was provided by the National Science Foundation through the Presidential Young Investigator Program under Grant CHE-8552627. J.T.H. acknowledges a Dreyfus Teacher-Scholar Award and a fellowship from the Alfred P. Sloan Foundation.

Department of Chemistry
Northwestern University
2145 North Sheridan Road
Evanston, Illinois 60208

Jody A. Roberts
Joseph T. Hupp*

Received August 9, 1991

Synthesis and Structural Characterization of a Novel S-Bridged $Co^{III}Ni^{II}Co^{III}$ Complex, $[Ni\{Co(aet)_2(en)\}_2]^{4+}$ (aet = 2-Aminoethanethiolate; en = Ethylenediamine): Ligand Transfer from the Nickel(II) to the Cobalt(III) Coordination Sphere

It has been recognized that the bridging ability of coordinated thiolato sulfur atoms allows *fac*(*S*)-$[M(aet)_3]$ or *fac*(*S*)-$[M(L\text{-cys-}N,S)_3]^{3-}$ (aet = 2-aminoethanethiolate; L-cys = L-cysteinate; M = Co(III), Rh(III), or Ir(III)) to function as a terdentate ligand to a variety of metal ions, forming linear-type[1,2] or cage-type[3] S-bridged polynuclear structures. For example, the reactions of *fac*(*S*)-$[Co(aet \text{ or } L\text{-cys-}N,S)_3]^{0 \text{ or } 3-}$ with Co(II) or Co(III) have produced S-bridged trinuclear complexes $[Co^{III}\{Co(aet \text{ or } L\text{-cys-}N,S)_3\}_2]^{3+ \text{ or } 3-}$ [1a,2a,e] and those with $[CoCl_3(triamine)]$ gave S-bridged dinuclear complexes $[Co\{Co(aet \text{ or } L\text{-cys-}N,S)_3\}(triamine)]^{3+ \text{ or } 0}$.[2g] On the other hand, $[M'(aet)_2]$ (M' = Ni(II) or Pd(II)) has been shown to function as a bidentate ligand to M'' = Ni(II), Pd(II), and Pt(II), forming S-bridged trinuclear complexes $[M''\{M'(aet)_2\}_2]^{2+}$.[4] These facts seem to indicate that an S-bridged dinuclear complex $[Co\{Ni(aet)_2\}(en)_2]^{3+}$ is possibly formed by the reaction of $[Ni(aet)_2]$ with $[CoCl_2(en)_2]^+$. However, this reaction gave a novel S-bridged $Co^{III}Ni^{II}Co^{III}$ trinuclear complex (**1**), in which the bidentate-*N*,*S* ligand aet does not chelate to Ni(II), but to Co(III). In this paper we describe the synthesis, characterization, and properties of **1**.

To a green suspension of $[Ni(aet)_2]$[4a] (1.0 g, 4.7 mmol) in water was added *trans*-$[CoCl_2(en)_2]Cl$ (2.7 g, 9.4 mmol). After the mixture had been stirred at room temperature for 2 h, the resulting red-brown complex (**1**) (0.42 g) was collected by filtration. Recrystallization of **1** from water gave dark red crystals,[5] one of which was used for X-ray structural analysis. **1** was also obtained using *cis*-$[CoCl_2(en)_2]Cl$ instead of *trans*-$[CoCl_2(en)_2]Cl$.

X-ray structural analysis of **1** revealed the presence of a discrete tetravalent complex cation, four chloride anions, and water molecules.[6] As shown in Figure 1, the complex cation consists of two octahedral *cis*(*S*)-$[Co(aet)_2(en)]^+$ subunits and one nickel atom. The nickel atom is coordinated by four thiolato sulfur atoms from the two terminal *cis*(*S*)-$[Co(aet)_2(en)]^+$ subunits, forming the linear-type S-bridged trinuclear structure. The central NiS_4 sphere is markedly distorted from square-planar to tetrahedral geometry, in which the NiS1S1′ and NiS2S2′ planes intersect to form dihedral angle of 16.2°. This is inconsistent with the square-planar geometry of the central NiS_4 sphere observed in the related S-bridged trinuclear complex $[Ni\{Ni(aet)_2\}_2]^{2+}$.[4c] Molecular model examinations reveal that this distortion decreases the cross-plane interaction between the aet chelate rings of the two C_2-*cis*(*S*)-$[Co(aet)_2(en)]^+$ subunits. The S-Ni-S "bite" angles (86.86 (4) and 86.80 (5)°) are larger than those found in $[Ni\{Ni(aet)_2\}_2]^{2+}$ (81.4 (2)°) and more close to the S-Ni-S "bite" angles of 90-92° observed in the mononuclear $[Ni^{II}(thiolato)_4]^{2-}$ complexes.[7d,g] The Ni-S bond lengths (2.208 (1) and 2.199 (1) Å) are within the range of 2.16-2.23 Å normally observed for the four-coordinated Ni(II) complexes.[4c,7]

Of 10 isomers possible for $[Ni\{Co(aet)_2(en)\}_2]^{4+}$,[8] crystal **1** consists of the $\Delta(C_2\text{-}cis(S))\text{-}\Delta(C_2\text{-}cis(S))$ isomer and its enantiomer $\Lambda(C_2\text{-}cis(S)\text{-}\Lambda(C_2\text{-}cis(S))$, which combine to form the racemic compound (Figure 1). This is in agreement with the fact that **1** was optically resolved with use of $[Sb_2(d\text{-tart})_2]^{2-}$ as the

(1) (a) Bush, D. H.; Jicha, D. C. *Inorg. Chem.* **1962**, *1*, 884. (b) Brubaker, G. R.; Douglas, B. E. *Inorg. Chem.* **1967**, *6*, 1562. (c) DeSimone, R. E.; Ontko, T.; Wardman, L.; Blinn, E. L. *Inorg. Chem.* **1975**, *14*, 1313. (d) Blinn, E. L.; Butler, P.; Chapman, K. M.; Harris, S. *Inorg. Chim. Acta* **1977**, *24*, 139. (e) Heeg, M. J.; Blinn, E. L.; Deutsch, E. *Inorg. Chem.* **1985**, *24*, 1118. (f) Johnson, D. W.; Brewer, T. R. *Inorg. Chim. Acta* **1988**, *154*, 221.

(2) (a) Konno, T.; Aizawa, S.; Okamoto, K.; Hidaka, J. *Chem. Lett.* **1985**, 1017. (b) Okamoto, K.; Aizawa, S.; Konno, T.; Einaga, H.; Hidaka, J. *Bull. Chem. Soc. Jpn.* **1986**, *59*, 3859. (c) Aizawa, S.; Okamoto, K.; Einaga, H.; Hidaka, J. *Bull. Chem. Soc. Jpn.* **1988**, *61*, 1601. (d) Miyanowaki, S.; Konno, T.; Okamoto, K.; Hidaka, J. *Bull. Chem. Soc. Jpn.* **1988**, *61*, 2987. (e) Konno, T.; Aizawa, S.; Hidaka, J. *Bull. Chem. Soc. Jpn.* **1989**, *62*, 585. (f) Konno, T.; Aizawa, S.; Okamoto, K.; Hidaka, J. *Bull. Chem. Soc. Jpn.* **1990**, *63*, 792. (g) Konno, T.; Okamoto, K.; Hidaka, J. *Bull. Chem. Soc. Jpn.* **1990**, *63*, 3027.

(3) (a) Konno, T.; Okamoto, K.; Hidaka, J. *Chem. Lett.* **1990**, 1043. (b) Konno, T.; Okamoto, K.; Hidaka, J. *Inorg. Chem.* **1991**, *30*, 2253.

(4) (a) Jicha, D. C.; Busch, D. H. *Inorg. Chem.* **1962**, *1*, 872. (b) Jicha, D. C.; Busch, D. H. *Inorg. Chem.* **1962**, *1*, 878. (c) Wei, C. H.; Dahl, L. F. *Inorg. Chem.* **1970**, *9*, 1878.

(5) Anal. Calcd for $[Ni\{Co(NH_2CH_2CH_2S)_2(NH_2CH_2CH_2NH_2)\}_2]Cl_4 \cdot 6H_2O$: C, 16.93; H, 6.16; N, 13.16; Co, 13.85; Ni, 6.89. Found: C, 16.93; H, 6.15; N, 12.97; Co, 13.54; Ni, 6.56. Visible-UV spectrum, H_2O solvent [ν_{max}, 10^3 cm^{-1} (log ϵ; ϵ in mol^{-1} dm^3 cm^{-1})]: 21.1 (3.27 sh), 24.1 (3.69 sh), 27.78 (4.31), 37.31 (4.33), 42.02 (4.52). The sh label denotes a shoulder. NMR (500 MHz, D_2O, ppm from DSS): ^1H NMR, δ 1.78 (td, J = 14 and 5 Hz, $-CH_2S$), 2.50 (dd, J = 14 and 4 Hz, $-CH_2S$), 2.54 (d, J = 9 Hz, $-CH_2N$ of en), 2.77 (d, J = 9 Hz, $-CH_2N$ of en), 3.67 (dd, J = 13 and 4 Hz, $-CH_2N$), 4.31 (td, J = 13 and 4 Hz, $-CH_2N$); ^{13}C NMR, δ 34.70 ($-CH_2S$), 46.58 ($-CH_2NH_2$ of en), and 55.76 ($-CH_2NH_2$).

(6) Crystal data for $[Ni\{Co(C_2H_6NS)_2(C_2H_8N_2)\}_2]Cl_4 \cdot 6H_2O = C_{12}H_{52}N_8O_6S_4Cl_4Co_2Ni$ at 293 K: M_r = 851.2, 0.23 × 0.20 × 0.15 mm, monoclinic, $C2/c$, a = 14.987 (4) Å, b = 19.480 (3) Å, c = 12.916 (4) Å, β = 113.67 (1)°, V = 3454 (1) Å^3, Z = 4, D_{calcd} = 1.64 g cm^{-3}, λ(Mo Kα) = 0.71069 Å, μ(Mo Kα) = 20.75 cm^{-1}, R (R_w) = 0.046 (0.065) for 2875 independent reflections with $F_o > 3\sigma(F_o)$ ($2\theta < 50°$). The position of the nickel atom was obtained from a three-dimensional Patterson function. Difference Fourier maps, based on the nickel position, revealed all the non-hydrogen atoms. The Co1, Ni, and Co2 atoms were constrained to the special positions of point symmetry 2 (0, y, 0.25) with a site occupancy factor of 0.5. Two of three water oxygen atoms (OW2 and OW3) exhibited positional disorder and were best modeled with two positions for each atom. The structure was refined by full-matrix least-squares methods using anisotropic thermal parameters for non-hydrogen atoms. All calculations were performed with use of the programs of SHELX-76. Selected bond lengths (Å) and angles (deg) are as follows: Ni-S1, 2.208 (1); Ni-S2, 2.199 (1); Co-S1, 2.233 (1); Co-S2, 2.242 (1), Co1-N11, 1.969 (3); Co1-N12, 1.987 (3); Co2-N21, 1.987 (3); Co2-N22, 2.003 (3); S1-Ni-S1′, 86.86 (4); S1-Ni-S2, 94.24 (4); S2-Ni-S2′, 86.80 (5); S1-Co1-S1′, 85.64 (5); S1-Co1-N11, 87.7 (1); S1-Co1-N12, 94.8 (1); N11-Co1-N12, 91.5 (1); N12-Co1-N12′, 85.0 (2); S2-Co2-S2′, 84.74 (4); S2-Co2-N21, 87.5 (1); S2-Co2-N22, 95.0 (1); N21-Co2-N22, 91.9 (1); N22-Co2-N22′, 85.4 (2).

(7) (a) Snyder, B. S.; Rao, C. P.; Holm, R. H. *Aust. J. Chem.* **1986**, *39*, 963. (b) Tremel, W.; Kriege, M.; Krebs, B.; Henkel, G. *Inorg. Chem.* **1988**, *27*, 3886. (c) Kruger, H.-J.; Holm, R. H. *Inorg. Chem.* **1989**, *28*, 1148. (d) Fox, S.; Wang, Y.; Silver, A.; Millar, M. *J. Am. Chem. Soc.* **1990**, *112*, 3218. (e) Turner, M. A.; Driessen, W. L.; Reedijk, J. *Inorg. Chem.* **1990**, *29*, 3331. (f) Mills, D. K.; Reibenspies, J. H.; Darensbourg, M. Y. *Inorg. Chem.* **1990**, *29*, 4368. (g) Sellmann, D.; Funfgelder, S.; Pohlmann, G.; Knoch, F.; Moll, M. *Inorg. Chem.* **1990**, *29*, 4772. (h) Martin, E. M.; Bereman, R. D.; Singh, P. *Inorg. Chem.* **1991**, *30*, 957.

(8) Considering two absolute configurations (Δ and Λ) and two geometries (C_1-*cis*(*S*) and C_2-*cis*(*S*)) for the two *cis*(*S*)-$[Co(aet)_2(en)]^+$ subunits, the possible isomers are $\Delta(C_1\text{-}cis(S))\text{-}\Delta(C_1\text{-}cis(S))$, $\Delta(C_1\text{-}cis(S))\text{-}\Delta(C_2\text{-}cis(S))$, $\Delta(C_2\text{-}cis(S))\text{-}\Delta(C_2\text{-}cis(S))$, $\Delta(C_1\text{-}cis(S))\text{-}\Lambda(C_1\text{-}cis(S))$, $\Delta(C_1\text{-}cis(S))\text{-}\Lambda(C_2\text{-}cis(S))$, $\Delta(C_2\text{-}cis(S))\text{-}\Lambda(C_1\text{-}cis(S))$, $\Delta(C_2\text{-}cis(S))\text{-}\Lambda(C_2\text{-}cis(S))$, $\Lambda(C_1\text{-}cis(S))\text{-}\Lambda(C_1\text{-}cis(S))$, $\Lambda(C_1\text{-}cis(S))\text{-}\Lambda(C_2\text{-}cis(S))$, $\Lambda(C_2\text{-}cis(S))\text{-}\Lambda(C_2\text{-}cis(S))$. The prefixes C_1 and C_2 denote that the *cis*(*S*)-$[Co(aet)_2(en)]^+$ subunit has a C_1 or C_2 axis.

0020-1669/92/1331-0160$03.00/0